

Causes and biogeochemical implications of regional differences in silicification of marine diatoms

Stephen B. Baines,¹ Benjamin S. Twining,² Mark A. Brzezinski,³ David M. Nelson,⁴ and Nicholas S. Fisher⁵

Received 27 April 2010; revised 10 September 2010; accepted 28 September 2010; published 24 December 2010.

[1] Diatoms facilitate the export of organic carbon and associated nutrient elements in the ocean because their dense opaline silica shells provide ballast to sinking particles. Marine ecosystem models generally assume that cellular silicification is either constant or varies solely due to physiological responses. Using a cell-specific technique, synchrotron-based X-ray fluorescence (SXRF) microscopy, we show that diatom cells in the cold, high-silicic-acid waters of the Antarctic Zone of the Southern Ocean (SOAZ) had 6 times more Si per volume than did those inhabiting the warm, low-silicic-acid waters of eastern equatorial Pacific (EEP). Ratios of Si:P and Si:S differed less than this because cellular P and S concentrations were higher in SOAZ cells. Resulting differences in excess density and frustule surface area-to-volume ratios should result in more efficient removal and slower dissolution of biogenic silica in the SOAZ compared to the EEP. Moreover, the difference between the excess densities of diatoms and nondiatoms was 15-fold greater in the SOAZ than in the EEP. Several possible causes of the regional differences in silicification are evaluated. Differences in cell volume between regions and additions of silicic acid and iron had minor effects on silicification. Instead, cellular silicification varied substantially among diatom morphological types within each region, suggesting that community composition largely determined the community silicification in these regions. We suggest that ecological processes may cause much larger systematic regional and temporal differences in cellular stoichiometry than is currently accommodated by ecosystem models.

Citation: Baines, S. B., B. S. Twining, M. A. Brzezinski, D. M. Nelson, and N. S. Fisher (2010), Causes and biogeochemical implications of regional differences in silicification of marine diatoms, *Global Biogeochem. Cycles*, 24, GB4031, doi:10.1029/2010GB003856.

1. Introduction

[2] Diatoms are believed to play a critical role in oceanic biogeochemical cycles because their siliceous cell walls impart substantial excess density, or mineral “ballast,” to large, fast sinking aggregates and herbivore feces that contain them [Armstrong *et al.*, 2002; Buesseler, 1998]. Consequently, biogeochemical models that link the supply of

nutrients such as Fe and nitrate to the depletion and recycling of nutrient elements or to the sequestration of C in the deep ocean often explicitly model the response of diatoms separately from other primary producers [Jin *et al.*, 2006; Moore *et al.*, 2004; Salihoglu and Hofmann, 2007]. These “ecosystem models” recognize differences in elemental composition of functional groups within the plankton. However, they also often assume that diatoms themselves have a nearly fixed elemental composition, and therefore fixed silica content and Si:N requirement, across the oceans. While the effect of varying nutrient concentrations of silica and nitrogen content in marine diatoms in response to silicic acid and Fe can be modeled, such physiologically based approaches still assume that all diatoms respond to such variations in a uniform manner [Mongin *et al.*, 2006]. Such physiological effects are presumed to be responsible for large regional differences in ratios of silicic acid and nitrate use across the ocean and in Si:N ratios of suspended and sinking particulate material [Dunne *et al.*, 1999; Hutchins and Bruland, 1998; Mongin *et al.*, 2006; Sarmiento *et al.*, 2004]. Variations in the dissolution or mineralization of silica and

¹Department of Ecology and Evolution, Stony Brook University, Stony Brook, New York, USA.

²Bigelow Laboratory for Ocean Sciences, West Boothbay Harbor, Maine, USA.

³Marine Science Institute and the Department of Ecology, Evolution and Marine Biology, University of California, Santa Barbara, California, USA.

⁴Institut Universitaire Européen de la Mer, Technopôle Brest-Iroise, Plouzané, France.

⁵School of Marine and Atmospheric Sciences, Stony Brook University, Stony Brook, New York, USA.

organic nitrogen have also been invoked to explain these patterns [Bidle *et al.*, 2002; Brzezinski *et al.*, 2003; Dugdale and Wilkerson, 1998].

[3] What remains unaccounted for in biogeochemical models is the large amount of interspecific variation in the Si content of diatoms. Marine diatom species in culture range in volume-normalized cellular silica content, here termed silicification, by over an order of magnitude [Conley *et al.*, 1989]. Marine species exhibit an order of magnitude lower silicification on average than freshwater species, suggesting strong selection on silicification across the marine/freshwater divide [Conley *et al.*, 1989]. By comparison, physiological plasticity within individual species is much less pronounced. Silicification generally varies by a factor of 4 or less within cultured species in response to limitation by silicic acid [Brzezinski, 1985; Paasche, 1973]. As pointed out in recent reviews [Marchetti and Cassar, 2009; Sarthou *et al.*, 2005], a number of studies have shown that Fe availability can cause cellular ratios of Si:N to vary by a factor of 2–4 within diatom species in culture [Marchetti and Harrison, 2007; Takeda, 1998; Timmermans and van der Wagt, 2010; Timmermans *et al.*, 2004] and the field [Baines *et al.*, 2010; Twining *et al.*, 2004]. The effect of Fe on cellular Si:N ratios has been linked to shifts in community nitrate:silicate uptake ratios in situ [Coale *et al.*, 2004; Franck *et al.*, 2000, 2003; Hoffmann *et al.*, 2006; Hutchins and Bruland, 1998]. Culture studies [Takeda, 1998; Timmermans *et al.*, 2004; Marchetti and Harrison, 2007] and cell-specific analyses of field samples [Baines *et al.*, 2010; Twining *et al.*, 2004] show that the variability in Si:N ratios in cells not only reflects differences in silicification, but also the effect of Fe on cell organic matter content. Indeed, changes to silica content per volume in response to Fe limitation are usually less than a factor of 3 [Hoffmann *et al.*, 2007; Marchetti and Harrison, 2007; Marchetti *et al.*, 2010; Takeda, 1998; Twining *et al.*, 2004]. Because of the large amount of interspecific variability in silicification, environmental conditions that favor species on the basis of their level of silicification have the potential to cause much greater variation in community silica content than can physiological responses alone. The variability among species may also amplify or obscure physiologically based differences.

[4] To determine whether biogeochemically significant, taxonomically based variation in diatom silicification is evident in natural plankton communities, we used synchrotron-based X-ray fluorescence microscopy (SXRF) [Twining *et al.*, 2003] to measure the Si content of individual diatom cells collected from two important Fe-limited HNLC regions that differ in silicic acid availability, temperature and light. The Southern Ocean south of the Antarctic Polar Front (referred to here as the Southern Ocean Antarctic Zone, or SOAZ) is characterized by near-freezing water temperatures, poor-density stratification, vigorous wind-driven turbulent mixing, low light intensities and high silicic acid concentrations [Coale *et al.*, 2004]. The region appears to play an important role in regulating global atmospheric CO₂, while the substantial deposition of biogenic silica in sediments underlying the region limits the supply of silicic acid to the rest of the ocean [Marinov *et al.*, 2006; Pondaven *et al.*, 2000; Sarmiento *et al.*, 2004]. The

eastern equatorial Pacific (EEP) is the largest natural source of CO₂ to the atmosphere [Takahashi *et al.*, 1997] and is characterized by warmer water, strong permanent density stratification, calm surface conditions and much lower dissolved silicic acid concentrations [Chai *et al.*, 2002]. Upwelling of nutrients is more modest and less seasonal, resulting from both the continuous effect of Ekman divergence along the equator, and the periodic passage of tropical instability waves [Foley *et al.*, 1997; Strutton *et al.*, 2001, 2010].

[5] We use our data to determine the degree to which diatom Si, P and S content vary between these two important Fe-limited regions. We then assess whether any differences are the result of physiological responses to the different environments, or differences in community composition and cell size. Finally we use our measurements to estimate how species composition can affect regional differences in sinking and dissolution of silica within aggregates or fecal pellets.

2. Materials and Methods

2.1. Sampling Sites

[6] Cells from the Southern Ocean were collected during the Southern Ocean Fe experiment (SOFEX) as described by Twining *et al.* [2004]. This part of the experiment involved four successive additions of Fe to a 15 km² × 15 km² patch at 66°S 172°W, which was positioned south of the Antarctic polar front. Nutrient concentrations at the initiation of the experiment were 2 μM phosphate, 30 μM nitrate and 65 μM silicic acid. Samples were collected from the patch 0.7 d prior to the initial fertilization (Pre), 3.2 days after the first addition (Fe-1), and 3.0 days after the second addition (Fe-2). In addition, a sample was taken from a reference station outside the fertilized patch 7 d after the initial fertilization (Out). The data presented here differ from those presented previously [Twining *et al.*, 2004] in two important respects. First, we have categorized all of the cells into types based on their morphology. Second, we employ a new method for quantifying P and S from SXRF data [Núñez-Milland *et al.*, 2010] that was also applied to the EEP diatoms, facilitating direct comparisons between the regions. The equatorial Pacific diatoms were collected as part of two equatorial biocomplexity cruises in December 2004 (EB04) and September 2005 (EB05) [Nelson and Landry, 2010]. The first cruise consisted of a meridional transect from 4°N to 4°S at 110°W, and a zonal transect along the equator from 116.7°W to 140°W. The second cruise consisted of a latitudinal transect from 4°N to 2.5°S at 140°W and a zonal transect along 0.5°N between 132.5°W to 125°W. Samples for SXRF analyses were collected at 10 stations during EB04 and 6 stations during EB05. To assess sensitivity of cellular elemental contents to nutrient conditions, we also collected samples from three deck-board microcosms to which 2 nmol L⁻¹ Fe or 20 μmol L⁻¹ silicic acid were added [Brzezinski *et al.*, 2010].

2.2. SXRF Methods

[7] To prepare samples, 40 mL of seawater was preserved with electron microscopy grade 10% glutaraldehyde to a final concentration of 0.25%. The samples were then centrifuged

using a swing out rotor for 30 min at 438g so as to sediment cells onto Au-carbon formvar coated London Finder electron transmission microscopy grids (Electron Microscopy Sciences) that were mounted on flat araldite resin inserts within the centrifuge tubes. Samples were air-dried in the dark and imaged under epifluorescence on the ship to facilitate later identification of cell types. For samples from low-Fe waters, virtually all diatoms on the grids were analyzed. Under high-Fe conditions cell types were analyzed in rough proportion their relative abundance on the grids.

[8] X-ray fluorescence analyses were conducted at the 2-ID-E beamline of the Advanced Photon Source, Argonne National Laboratory, Argonne, Illinois. The excitation beam energy was ~ 10 keV. Depending on beamline conditions and the particular optics (Fresnel zone-plates) employed, spatial resolution ranged from 0.25 to 0.7 μm . Full X-ray emission spectra (1–10 keV) collected using an energy-dispersive Ge detector were summed over the area of the cell and over a representative background region. Quantification of cellular Si was achieved by use of National Institute of Standards and Technology standards (NBS1832/1832) using previously described fitting procedures [Twining *et al.*, 2003; Vogt, 2003]. No reliable standards exist for sulfur (a proxy for protein) and phosphorus, so fluorescence yields for these elements were interpolated from regressions of empirical fluorescence yields for all other elements in the NIST standards on the theoretical fluorescence yields calculated for those elements given the excitation energy used. These regressions were always linear with r^2 values >0.99 . SXRF measurements of cellular phosphorus in the diatom *Thalassiosira pseudonana* made using this method were within 25% of bulk colorimetric measurements made on the same culture and well within the range of values reported in the literature for this species [Nuñez-Milland *et al.*, 2010].

2.3. Estimates of Cell Biovolume and Surface Area

[9] Measurements of cellular linear dimensions were made with a light microscope (Leica DMI 6300) using Image Pro analysis software. Cell biovolumes (V_{cell}) and cell surface areas (SA_{cell}) were calculated using standard geometric formulae [Hillebrand *et al.*, 1999]. Centric diatoms were presumed to approximate cylinders. When measured in girdle view, the dimension parallel to the girdle lines was presumed to equal to the valve face diameter (D), and that perpendicular to the girdle lines was assumed to equal the height (H). When measured in valve view, H was presumed to equal D divided by 1.45, which was the average ratio of valve diameter to cylinder height in girdle view diatoms. In most cases, pennate diatoms were presumed to approximate ellipsoid prisms. We assumed that transapical widths in girdle and valve view were equivalent, a rule of thumb that was found to hold well for *Fragilariopsis cylindrus* in the Southern Ocean samples, which were present in both valve and girdle view. Because of its unique shape, the biovolume of this most common pennate in the Southern Ocean samples was approximated based on a rod shaped prism, with the rounded ends described as semi-ellipsoids whose radii combined comprised 5% of the length of the cell.

[10] Precise identification of the species was impeded by the use of dry optics in our microscopy. Such optics have

reduced resolution compared to wet or oil optics or electron microscopy, making it difficult to resolve fine-scale features and often preventing identification. However, wet samples cannot be analyzed using SXRF because of the large interferences associated with Cl^- ions in solution and the potential for radiation damage to the cells. Likewise, coating of samples for electron microscopy would have compromised our element analysis. Thus, the genus and species names we have assigned to our morphological types, where noted, are tentative.

2.4. Data Filtering

[11] The presence of physiologically compromised cells and quantification problems stemming from interference among elemental fluorescence peaks can compromise SXRF measurements. While our spectral modeling normally corrects for modest levels of spectral interference, poor P, S and Si quantification can occur in cells that lie too near the grid bars of the Au transmission electron microscope grids because of the Au m-line at 2.212 keV. To identify cells that were either moribund or subject to such interference, we made a priori decisions to exclude cells from analyses for which measurements for any one of the three target elements (Si, P and S) could not be made. Negative background-corrected peak areas were automatically discarded, as were any peaks areas that were less than a factor of 5 greater than the statistical uncertainty around the peak area estimate for the cell. In addition, data were screened for outliers by first running an analysis of covariance (ANCOVA) model that corrected for differences among regions, stations, diatom morphological type and cell volume. Cells for which Si, S and P content were 3.5 standard deviations away from the mean were labeled as outliers and excluded from all subsequent analyses. Given a normal distribution and 110 observations, there is only a 5% chance for any observation to exceed this threshold. Using this procedure, 12 of 143 cells were removed.

2.5. Statistical Analyses of SXRF Data

[12] Analysis of variance (ANOVA) and covariance (ANCOVA) were used to determine the importance of various predictor variables in determining cellular elemental concentrations ($\text{mol } \mu\text{m}^{-3}$) under low-Fe conditions. All continuous variables had to be log-transformed to meet the assumptions of normality and homogeneity of variance in the residuals. Due to the number of comparisons made, the significance of all explanatory factors were determined using t tests with a significance threshold of $p = 0.01$ so as to limit false positive results. Values between 0.05 and 0.01 are referred to as marginally significant. The relative effectiveness of each factor was assessed by comparing the amount of variance explained (r^2) in analyses containing that factor to those that did not. The main categorical predictor was REGION (treatment levels = SOAZ and EEP). Because there were no cell types in common between the regions, the categorical predictor variable, TYPE, was a factor nested within REGION. Significance for this variable therefore indicates that a nonrandom amount of variability within regions could be ascribed to differences among cell types. VOLUME was also used as continuous factor to correct for

Table 1. Mean Cell Dimensions and Elemental Content of Diatom Morphological Types From the Two Regions^a

Cell Type Description	Code	<i>N</i>	Length	Width	Volume	[Si] _{cell}	[P] _{cell}	[S] _{cell}	Si:P	Si:S	S:P
<i>Eastern Equatorial Pacific</i>											
<i>Chaetoceros concavicornis</i>	c1	2	14.4 (1)	6.5	479 (32)	0.38 (0.1)	28 (1.4)	38 (14)	13.5 (1.7)	11.2 (3.3)	1.4 (0.5)
<i>Thalassiosira sp.</i>	c2	3 (2)	5.1 (1.1)	3.5 (0.5)	55 (21)	3.36 (1.2)	105 (25)	173 (68)	36.8 (7.3)	21.1 (4.4)	1.7 (0.7)
Large centric	c3	1	11.9	10.9	1110	0.72	22	18	33.1	40.5	0.8
<i>Chaetoceros sp.</i>	c4	1	6.7	4.8	122	1.4	51	119	27.5	11.7	2.4
<i>Nitzschia bicipitata</i>	p1	8 (7)	8.2 (0.6)	3.8 (0.1)	93 (10)	1.65 (0.1)	54 (10)	66 (8)	37.5 (5.4)	27.6 (3.5)	1.5 (0.2)
<i>Nitzschia sp.</i>	p2	2	45.6 (4.2)	8.2 (4.7)	3461 (3051)	0.61 (0.4)	9 (4)	33 (23)	60.1 (22.9)	18 (0.7)	3.3 (1.1)
<i>Pseudo-nitzschia sp1</i>	p3	44 (38)	23.6 (0.7)	2.3 (0.1)	102 (8)	0.66 (0.1)	33 (4)	71 (11)	20.2 (1.2)	11.4 (0.8)	2.2 (0.3)
<i>Pseudo-nitzschia sp2</i>	p4	30 (27)	10.6 (0.3)	2.4 (0.1)	47 (3)	0.64 (0.1)	44 (5)	59 (4)	15.6 (1.6)	11.6 (0.8)	1.5 (0.2)
Thin pennate	p5	1	41.7	2.4	184	0.51	12	4	43.2	125.1	0.3
Thin pennate	p9	1 (0)	58.1	1.4	91	1.78		98		18.2	
Robust pennate	p10	1 (0)	25	4.9	467	2.34		47		50.3	
<i>Southern Ocean</i>											
Medium centric	c1	7 (6)	7.2 (0.6)	5.1 (0.4)	229 (58)	2.31 (0.27)	56 (5)	70 (6)	41.2 (8.2)	34.1 (4.7)	1.3 (0.1)
Large centric	c2	2	14.4 (2.3)	12.4 (4)	1539 (1059)	15.45 (5.05)	132 (56)	104 (52)	122.9 (14.1)	166.5 (35.2)	0.8 (0.1)
Small centric	c3	11	5.4 (0.3)	4.1 (0.3)	104 (18)	1.9 (0.08)	69 (9)	85 (14)	33.7 (5)	29 (4.6)	1.2 (0.1)
Large dark centric	c5	3	11.5 (1.9)	8.9 (1.3)	994 (507)	4.48 (2.18)	134 (64)	138 (62)	29.4 (10.3)	26 (6.8)	1.1 (0.1)
<i>Chaetoceros sp.</i>	c6	1	8.5	4.4	247	2.79	9	14	670.9	467.9	1.4
<i>Fragilariopsis cylindrus</i>	p1	21	22.5 (0.9)	9.7 (0.4)	2174 (227)	4.12 (0.27)	119 (22)	78 (5)	53.2 (7.1)	54.9 (3.5)	0.9 (0.1)
<i>Navicula sp.</i>	p2	1	59.8	8.8	3607	2.8	57	52	49.3	53.8	0.9
Small ovoid pennate	p3	2	8.1 (0.7)	4.6 (0.1)	137 (15)	1.54 (0.05)	75 (6)	112 (2)	20.5 (1.1)	13.8 (0.2)	1.5 (0.1)
Small rectangular pennate	p4	3 (2)	8.7 (0.5)	4.7 (0.4)	151 (27)	4.07 (0.93)	57 (14)	88 (5)	94.7 (38.9)	48 (13.5)	1.5 (0.3)

^aCell type descriptions are provisional taxonomic designations (in italics) or morphological descriptions. IDs beginning with the letter “c” are centric diatoms while those beginning with the letter “p” are pennates. Averages include cells collected from low-Fe conditions in the EEP and SOAZ, and high-Fe conditions in the SOAZ. Length and width are in μm , and volume is in μm^3 . Cellular concentrations of Si ([Si]_{cell}) are in mol L^{-1} , while cellular concentrations of P ([P]_{cell}) and S ([S]_{cell}) are in mmol L^{-1} . Elemental ratios are mol mol^{-1} . Values in parentheses are standard errors the difference between observations when only two representatives for a morphological type were measured. *N* is the number of cells used to calculate means, with values in parentheses being the number used for P related variables. Fewer cells were used for the latter cases because of poor quantification during the December 2005 SXRF run.

effects of cell size on cellular elemental concentrations. We tested for significance of the interactions between VOLUME and REGION to determine if the relationship between cellular composition and VOLUME were the same between the two regions. Region-specific analyses were also conducted to determine if the variance explained by different factors varied among regions.

[13] To estimate effects of Fe on cellular composition in the SOAZ, we also analyzed data taken before and after Fe addition during SOFEX. There were three levels of Fe exposure: Low Fe, High Fe-1 (after first Fe addition), and High Fe-2 (after second Fe addition). The effect of Fe on cellular composition in the EEP was assessed determining if dissolved Fe concentrations (averaged over 0–60 m, the typical depth of the mixed layer) were correlated to cellular S, P and Si concentrations after correcting for cell type and volume effects. Cellular Si, P and S concentrations were also compared between control, +Si (20 nmol L^{-1}) and +Fe (2 nmol L^{-1}) treatments in the 4–5 d deckboard microcosm experiments [Baines *et al.*, 2010; Brzezinski *et al.*, 2010]. Response to silicic acid and Fe addition were tested using paired *t* tests among treatments within an experiment. Data from time points which experienced nutrient depletion were excluded.

2.6. Nutrient Use Ratios in the EEP

[14] We estimated diatom nutrient use ratios in the EEP from changes in concentrations of phosphate, nitrate and silicic acid within the deckboard experiments. This approach was justified by two lines of evidence indicating that dia-

toms were primarily responsible for increases in biomass within the experiments [Brzezinski *et al.*, 2010]. First, exposure to better light conditions resulted in significant increases in chlorophyll over the first 48 h in all treatments except those to which Ge, a known inhibitor of diatom silica production, was added. Second, microscopy revealed that significant differences in biovolume among experimental treatments were only observed for diatoms [Brzezinski *et al.*, 2010]. The depletion ratios were determined by dividing the range of concentrations observed for one nutrient over that of another, as this approach is robust to transient initial increases due to death and decomposition of cyanobacteria that were inhibited by the high-light environment of the microcosms. We excluded observations for which silicic acid and nitrate + nitrite were $<0.1 \mu\text{mol L}^{-1}$, or phosphate was $<0.05 \mu\text{mol L}^{-1}$ to limit effects of lowered nutrient levels on nutrient uptake.

3. Results

3.1. Summary of Analyzed Cells

[15] A total of 51 diatoms representing 9 morphological types were from the SOAZ, with 18 of these being collected from low-Fe sites (Table 1). These cells were evenly divided between pennates (24 individuals, 4 types) and centrics (27 individuals, 5 types). Another 93 diatoms representing 11 types are from the two EEP cruises, with pennates comprising the vast majority of cells (88 individuals, 7 types) and centrics a small minority (7 individuals, 3 types). In both regions, only 3 morphological types were represented by

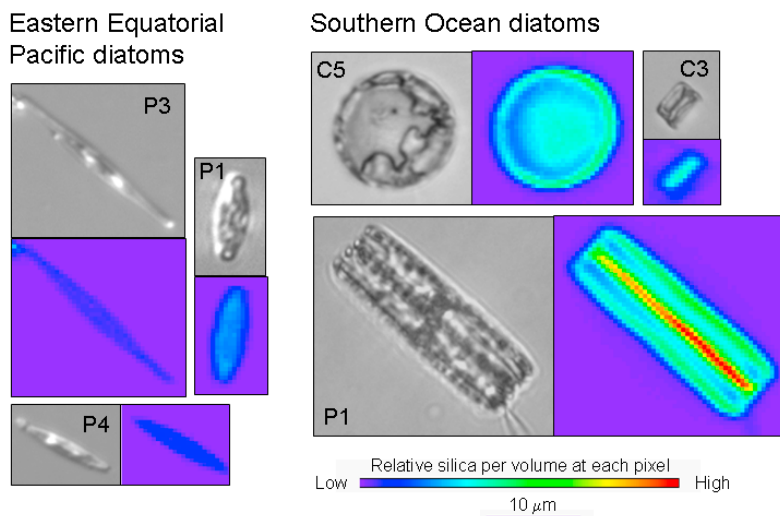


Figure 1. Differential interference contrast micrographs and false color maps of Si X-ray fluorescence for the three most common diatom taxa from the (left) eastern equatorial Pacific (EEP) and (right) Southern Ocean–Antarctic Zone (SOAZ). The fluorescence scale and linear dimensions are the same for all images to emphasize differences in size and Si content among taxa.

more than 3 individuals. In the SOAZ, the main pennate was *Fragilariopsis cylindrus* (SOAZ-p1), while the two centric diatoms (SOAZ-c1 and SOAZ-c3) were unidentified but probably were members of the genus *Thalassiosira* (Figure 1). In the EEP, the two most common pennate diatoms belong to the genus *Pseudo-nitzschia* (EEP-p3 and EEP-p4) while the third smaller pennate diatom was identified tentatively as *Nitzschia bicapitata* (EEP-p1). The two *Pseudo-nitzschia* dominated the 10–40 μm size fraction in this region [Taylor *et al.*, 2010]. Because of their high growth rates, diatoms comprising this size fraction accounted for 60–100% of the biogenic silica production in the region [Krause *et al.*, 2010b]. Cells from the EEP were on average smaller in terms of biovolume, averaging 178 μm^3 , while cells from the SOAZ averaged 1158 μm^3 (Table 2). While the greatest axial dimension was almost the same in the two regions, the aspect ratio of diatoms in the EEP was more than a factor of 3.5 greater than that of the SOAZ diatoms, and the ratio of surface

area: volume of EEP diatoms was more than twice that of diatoms from the SOAZ.

3.2. Regional Differences in Elemental Contents

[16] Diatoms collected from the SOAZ prior to Fe addition were nearly a factor of 6 more silicified than those in the EEP (Table 2). Because the ratio of surface area:volume of EEP diatoms was 3.5-fold larger than in the SOAZ, the difference between regions is ~20-fold if Si content is normalized to cell surface area. The difference between regions alone explains 52% of the variance in cellular silicification (Table 3). Cellular P concentrations in diatoms from the SOAZ were double those in diatoms from the EEP (Table 2), accounting for 21% of the variance in cellular P concentrations under low-Fe conditions (Table 3). Cellular S concentrations were only 30% higher in the SOAZ (Table 2), a difference that was only marginally significant ($p = 0.02$, t test) and which explained less than 5% of the variance

Table 2. Summary of Average Dimensions (μm), Volumes (μm^3), and Elemental Concentrations for All Diatom Cells Collected in the Eastern Equatorial Pacific and the Southern Ocean–Antarctic Zone^a

Region	Fe Level	Length	Width	Volume	[C] _{cell} [*]			[Si] _{cell}			[P] _{cell}			[S] _{cell}		
					<i>n</i>	Mean	SE	<i>n</i>	Mean	SE	<i>n</i>	Mean	SE	<i>n</i>	Mean	SE
EEP 2004	Low Fe	16.4	2.7	96	59	10.7	0.2	59	0.7	0.06	57	40	3.3	59	54	4
EEP 2005	Low Fe	20.8	3.2	323	34	10.2	0.3	34	0.9	0.18	24	38	6.9	34	81	11
EEP All	Low Fe	18.1	2.8	178	93	10.5	0.2	93	0.8	0.08	81	40	3.0	93	64	5
SOAZ	Low Fe	17.4	8.0	1246	19	7.1	0.4	19	4.9	1.0	18	82	11	19	82	6
SOAZ	High Fe-1	12.3	6.4	852	15	8.4	0.6	15	2.2	0.2	14	58	10	15	63	6
SOAZ	High Fe-2	14.3	7.3	1328	16	7.6	0.6	17	3.5	0.4	17	136	26	17	102	13

^aCarbon concentrations, [C]_{cell}^{*}, are estimated from cell volume based on equations found in the work of Menden-Deuer and Lessard [2000]. [P]_{cell} and [S]_{cell} are given in mmol (liter cell volume)⁻¹ while [Si]_{cell} and [C]_{cell}^{*} concentrations are given in mol (liter cell volume)⁻¹. “Low Fe” in the SOAZ represents diatoms collected from a patch prior to a mesoscale Fe fertilization and an adjacent unmanipulated patch sampled after the Fe fertilization. High Fe-1 and High Fe-2 refer to samples collected 3 days after the first and second Fe additions, respectively. Abbreviations are as follows: *n*, number of observations; SE, standard error.

Table 3. Summary Statistics for Analyses of Variance and Covariance of Cellular Elemental Composition Under Low-Fe Conditions^a

Variables	[Si]		[P]		[S]		Si:P		Si:S		S:P	
	<i>r</i> ²	<i>p</i>	<i>r</i> ²	<i>p</i>								
Region	0.52	<i><0.0001</i>	0.21	<i><0.0001</i>	0.05	<i>0.02</i>	0.39	<i><0.0001</i>	0.43	<i><0.0001</i>	0.08	<i>0.004</i>
Region		<i><0.0001</i>		<i><0.0001</i>		<i>0.06</i>		<i><0.0001</i>		<i><0.0001</i>		<i>0.50</i>
Cell type	0.83	<i><0.0001</i>	0.47	<i>0.001</i>	0.43	<i><0.0001</i>	0.68	<i><0.0001</i>	0.75	<i><0.0001</i>	0.31	<i>0.03</i>
Region		<i><0.0001</i>		<i><0.0001</i>		<i><0.0001</i>		<i>0.0003</i>		<i><0.0001</i>		<i>0.05</i>
Volume	0.53	<i>0.04</i>	0.37	<i><0.0001</i>	0.22	<i><0.0001</i>	0.44	<i>0.002</i>	0.46	<i>0.007</i>	0.08	<i>0.80</i>
Region		<i><0.0001</i>		<i><0.0001</i>		<i>0.01</i>		<i>0.003</i>		<i>0.001</i>		<i>0.51</i>
Volume		<i>0.507</i>		<i>0.0006</i>		<i>0.0003</i>		<i>0.006</i>		<i>0.004</i>		<i>0.42</i>
Region × volume	0.57	<i>0.003</i>	0.46	<i>0.0002</i>	0.26	<i>0.03</i>	0.44	<i>0.83</i>	0.47	<i>0.31</i>	0.11	<i>0.14</i>
Region		<i><0.0001</i>		<i><0.0001</i>		<i><0.0001</i>		<i>0.0007</i>		<i><0.0001</i>		<i>0.65</i>
Cell type		<i><0.0001</i>		<i>0.04</i>								
Volume	0.94	<i><0.0001</i>	0.66	<i><0.0001</i>	0.62	<i><0.0001</i>	0.68	<i>0.97</i>	0.75	<i>0.62</i>	0.31	<i>0.86</i>
Region		<i><0.0001</i>		<i>0.0007</i>		<i>0.04</i>		<i>0.79</i>		<i>0.26</i>		<i>0.51</i>
Cell type		<i><0.0001</i>		<i>0.0002</i>		<i><0.0001</i>		<i><0.0001</i>		<i><0.0001</i>		<i>0.07</i>
Volume		<i><0.0001</i>		<i><0.0001</i>		<i><0.0001</i>		<i>0.30</i>		<i>0.63</i>		<i>0.84</i>
Region × volume	0.95	<i>0.001</i>	0.66	<i>0.67</i>	0.62	<i>0.56</i>	0.69	<i>0.11</i>	0.75	<i>0.26</i>	0.31	<i>0.61</i>

^aAll continuous variables were log-transformed to meet assumptions of homogeneity of variance and normality. Listed is the proportion of variance explained by each model and the *p* value each predictor in that model (in italics). If adding the last predictor to the model improves the fit of the model (*p* < 0.01), the *r*² is also bolded.

(Table 3). As might be expected from these patterns, cellular S:P ratios differed between regions (*p* < 0.004, *t* test), averaging 1.2 in the SOAZ and 1.9 in the EEP across all cells. Because cellular concentrations of P and (to a lesser degree) S were all higher in the SOAZ, cellular Si:P and Si:S ratios did not differ between regions as much as did silicification. The average ratio of Si:P across all cells was a factor of ~3 greater in the SOAZ than in the EEP, and the ratio of average Si:S across all cells was a factor of ~4 greater (Table 4).

3.3. Differences Between Morphological Types

[17] Within regions, morphological type was the most important determinant of a cell's level of silicification.

Silicification varied by a factor of 6 among morphological types in the EEP and by an order of magnitude among morphological types in the SOAZ (Table 1). Accounting for both the regional difference and differences among types explained 83% of the variance in silicification under low-Fe conditions, compared to 52% when the regional difference alone was considered (Table 3). Taking each region separately, differences among morphological types accounted for 91% of the variance in silicification under low-Fe conditions in the SOAZ and 54% of the variance in the EEP. The average of the means for each cell type differed less among regions (by fourfold) than did the simple mean of all

Table 4. Elemental Ratios of Diatoms in the Southern Ocean–Antarctic Zone and Eastern Equatorial Pacific Estimated Using Different Approaches Under High and Low Fe^a

Region	Fe	Type of Data	Source	Si:P	Si:S	Si:N	Si:C
SOAZ	High	SXRF	this study	31 ± 6	36 ± 5	2.2 ± 0.5	0.31 ± 0.05
SOAZ	High	particulate matter	<i>Hoffmann et al.</i> [2007]	30		2.3	0.42
SOAZ	High	nutrient depletion	<i>Coale et al.</i> [2004]			2.1	
SOAZ	Ambient	SXRF	this study	67 ± 9	62 ± 9	4.2 ± 0.6	0.6 ± 0.08
SOAZ	Ambient	nutrient depletion	<i>Brzezinski et al.</i> [2003]			3.75	
SOAZ	Ambient	nutrient depletion	<i>Copin-Montegut and Copin-Montegut</i> [1978]			4	
SOAZ	Ambient	nutrient profiles	<i>Dunne et al.</i> [2007] (50°S–90°S)			4.5 ± 0.3 ^b	
EEP	High	SXRF	this study	14 ± 2.5 ^c	12.1 ± 2.5 ^c	0.76	0.114
EEP	High	nutrient depletion	this study	9.4 ± 2		0.38 ± 0.1	
EEP	High	nutrient depletion	<i>Coale et al.</i> [2004]			~1	
EEP	Ambient	SXRF	this study	22 ± 1.4	15 ± 1.5	1.1 ± 0.08	0.16 ± 0.01
EEP	Ambient	nutrient depletion	this study	9.6 ± 2		0.6 ± 0.1	
EEP	Ambient	nutrient profiles	<i>Dunne et al.</i> [1999]			0.75	
EEP	Ambient	nutrient profiles	<i>Dugdale and Wilkerson</i> [1998]			0.93	

^aSi:P, Si:S, Si:N and Si:C are cellular elemental ratios (mol mol⁻¹) ± 1 std error.

^bMean of averages a total of 9 means for 5° intervals from 70°S to 55°S determined separately for the Indian, Atlantic and Pacific sectors of the Southern Ocean.

^cBecause ratios for only one morphological type were measured in the mesocosms, the estimated ratios for the whole community are estimated by multiplying the ratios observed in field collected cells at ambient Fe by the ratio of elemental concentrations in the +Fe and control treatments of the deckboard microcosm experiments.

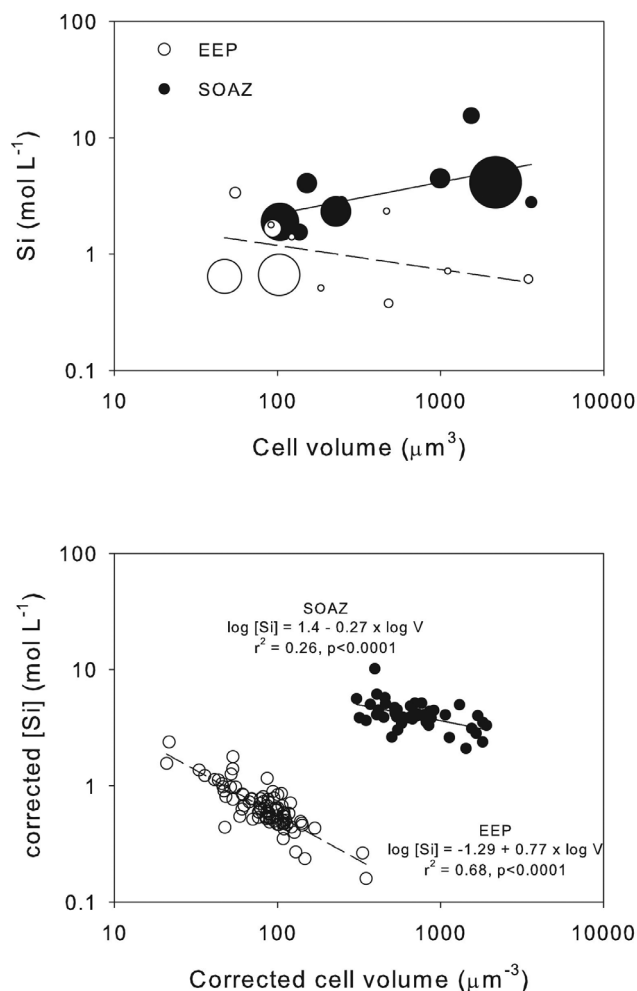


Figure 2. Effect of cell volume on silicification. In both cases the SOAZ data are in closed circles and EEP data in open circles, while solid and broken lines represent regressions for SOAZ and EEP data, respectively. (top) Averages of cell volume and cellular silicification for diatom morphological types. The size of the symbols is proportional to the number of observations for that species. (bottom) Individual observations of volume and silicification corrected for differences in average values for diatom morphological types and centered on the mean values for each region.

the cells analyzed (by sixfold). This discrepancy reflects the fact that those cell types that were less silicified than average were more numerous in the samples from the EEP.

[18] Cellular P and S concentrations also varied over an order of magnitude among morphological types, but much of the variability was due to rare types with low cellular P and S concentrations (Table 1). When only morphological types that were represented by ≥ 3 individuals were considered, cellular P and S concentrations varied by only a factor of 2 in the SOAZ, and by a factor of 2–3 in the EEP. Under low-Fe conditions, differences in cellular P concentrations among types accounted for nearly twice as much variance (47%) as did the regional difference alone (21%, $p = 0.001$,

Table 3). Regional differences in cellular S concentrations were small and only accounted for 5% of the variance in the data. In comparison, differences in cellular S concentration among morphological types accounted for almost an order of magnitude more variance (43%) than did the regional difference (5%, Table 3).

[19] Ratios of Si:P ($p < 0.001$) and Si:S ($p < 0.001$) varied significantly among morphological types (Table 1). In both cases, the high end of the range in ratios represents rare types with low cellular P and S. The Si:P and Si:S ratios of types represented by ≥ 3 individuals varied only by a factor of 2–3 within each region, ranging in the EEP from 15.6 to 37.5 and 11.6 to 27.6, respectively, and from 29 to 95 mol mol^{-1} and 26 to 55 mol mol^{-1} , respectively, in the SOAZ. Differences in the molar ratio of S:P among morphological types were only marginally significant ($p = 0.03$).

3.4. Effect of Cell Volume

[20] Cellular volume did not account for a large fraction of variance in silicification among morphological types and cannot account for the regional differences in silicification. Cell volume explained $< 20\%$ of the variance in silicification among morphological types in either region (Figure 2). A simple linear regression of cell volume on silicification using all the data from low-Fe sites accounted for only 20% of the variance in the data, compared to the 52% attributable to the regional difference (Table 3). Adding cell volume to a model that accounted for regional differences only increased the r^2 from 52% to 53%, with the effect of cell volume being only marginally significant ($p = 0.03$, Table 3). Allowing the relationship to have different slopes in the two regions also increased the r^2 marginally from 53% to 57% ($p = 0.001$, Table 3), but left the differences between regions highly significant ($p < 0.0001$).

[21] Cell volume was much more closely related to intraspecific variation in silicification than to interspecific variation. To visualize the intraspecific pattern, we first removed the interspecific variability in the silicification and cell volume data by subtracting the corresponding cell type mean from each observation. Because no cell types were shared among regions, this calculation centered the data from both regions on the origin making it difficult to visualize differences in trends between regions. Consequently, the corresponding regional means of silicification and cell volume were added to each observation to separate the data sets in graph space. The resulting plot shows that silicification values corrected for differences among types decline sharply and significantly with similarly corrected cell volumes (Figure 2). The slope of the relationship varied significantly between regions ($p = 0.001$, t test for interaction between REGION and VOLUME), being steeper by a factor of three in the EEP than in the SOAZ. As a consequence cell volume accounts for more variability in silicification in the EEP than it does in the SOAZ. In the EEP, 88% of the variance under low-Fe conditions could be accounted for by cell volume and differences among morphological types, while only 54% of the variance could be accounted for solely by differences among cell types. In the SOAZ under low-Fe conditions, almost 97% of the variance in cellular silicification could be explained by intraspecific differences in cell

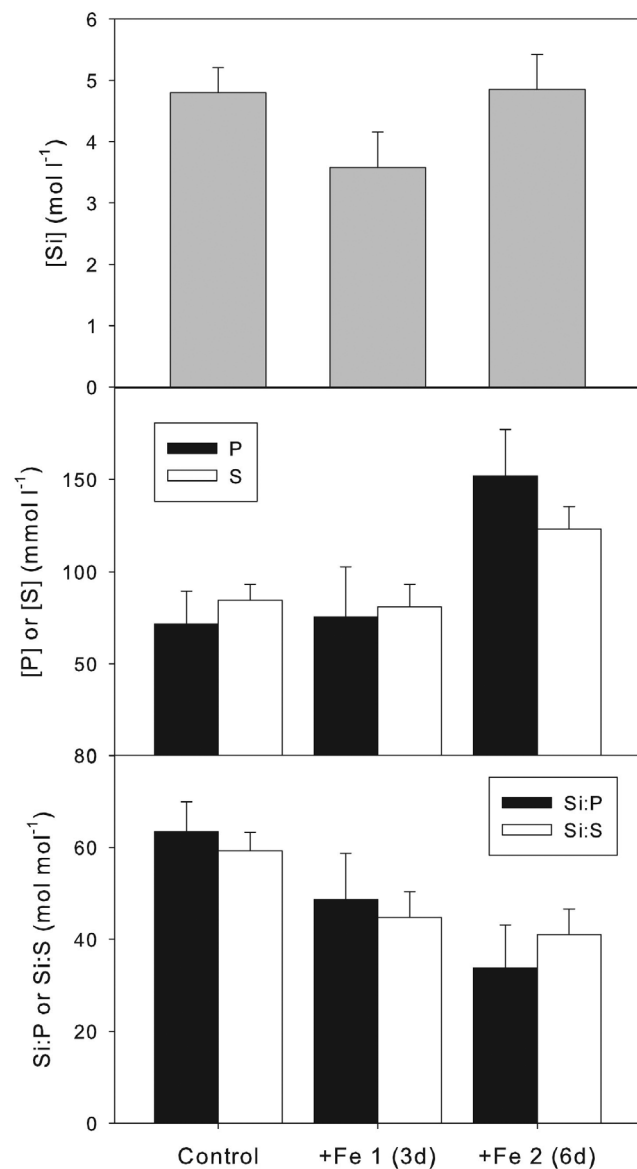


Figure 3. Effect of Fe addition on cellular elemental content of SOAZ diatoms during SOFEX: (top) silicification ($[\text{Si}]$, gray bars), (middle) cellular concentrations of P ($[\text{P}]$, black bars) and S ($[\text{S}]$, white bars), and (bottom) ratios of Si:P (black bars) and Si:S (white bars). Control, the experimental patch prior to fertilization and a reference station outside the patch after fertilization; +Fe 1 (3d), samples in the experimental patch 3 days after the first Fe addition; Fe-2 (6 d), samples in the experimental patch 6 days after the first Fe addition and 3 days after the second Fe addition. Values are detransformed least squared means determined from a one-way ANOVA of the logarithmically transformed data that corrected for differences in relative abundance of diatom morphological types. Bars are ± 1 SE.

volume and differences in silicification among morphological types.

[22] Cellular concentrations of S and P were also strongly related to cell volume, but only after accounting for regional differences and differences among morphological types (Table 3). Models accounting for cell volume, regional differences and differences among cell types explained 66% and 62% of the variance in P and S, respectively. However, ratios of S:P, Si:P and Si:S were unrelated to cell volume (Table 3).

3.5. Effects of Fe

[23] Ratios of Si:P and Si:S were lower after Fe addition in both regions, but changes in cellular silicification were either transient or driven by changes in cell volume rather than cellular Si content. Silicification of diatoms in the SOAZ initially declined by $\sim 50\%$ after the first Fe addition, but recovered to initial values after the second Fe addition (Figure 3). Cellular S and P concentrations increased by a factor of 2 from the beginning to the end of the experiment, causing a decline of $\sim 50\%$ in cellular Si:S and Si:P. In the EEP microcosm experiments, cellular silicification declined by $\sim 20\%$ after Fe addition relative to controls ($p = 0.005$, paired t test), while cellular P concentrations increased by $\sim 30\%$ ($p = 0.03$, paired t test) and cellular S concentrations remained unchanged. Given the aforementioned negative relationship between cell volume and cellular silicification in the EEP (Figure 2), the decline in silicification after Fe addition was expected because cell volume increased after Fe addition (Figure 4) [Baines *et al.*, 2010]. In contrast, cellular P and S concentrations after Fe addition were always greater than predicted by changes in cell volume, although variability among experiments made the increase in S insignificant. It is possible that the observed changes in cellular elemental concentration could reflect represent a shift in abundance among cryptic species contained within our morphological type designations. However, such a mechanism would only reinforce our interpretation of the results: that is, that physiological responses of silicification to Fe addition are small compared to differences among species.

[24] Analyses of field data agreed with the results from the experiments. Cellular silicification was not related to dissolved Fe in the upper mixed layer (0 – 60 m) in the EEP, and the slope was positive rather than negative (Table 5). However, cellular S ($p < 0.0001$) and cellular Si:S ($p = 0.005$) were significantly related to mixed layer dissolved Fe. The relationship between dissolved Fe and cellular P concentration was positive but insignificant. Cellular P concentrations were significantly related to both ambient phosphate concentrations ($p = 0.006$) and cellular S ($p < 0.0001$) in bivariate regressions. Because phosphate concentrations were negatively correlated with dissolved Fe in the EEP, the effect of phosphate on cellular P may have masked any effect of dissolved Fe on cellular P.

3.6. Effects of Silicic Acid

[25] Physiological responses to silicic acid could not explain why EEP diatoms exposed to relatively low silicic

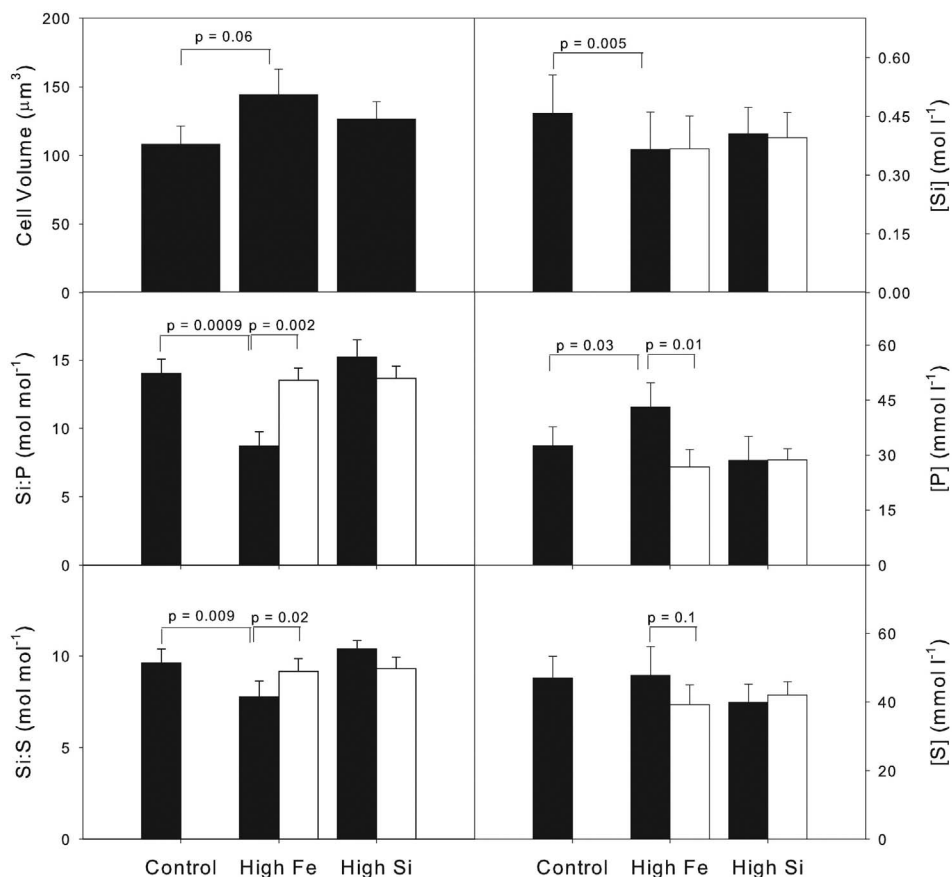


Figure 4. Effect of Fe and silicic acid additions on cellular elemental content of the diatom *Pseudonitzschia sp* (taxon is p1 in Figure 3) in three deckboard experiments during December 2004 and September 2005: (top left) cell volume, (top right) silicification ([Si]), cellular concentrations of (middle right) P ([P]) and (bottom right) S ([S]), and (bottom) ratios of Si:P and Si:S. Black bars are average of the three experiments \pm SE. Open bars are the predictions based on the dependency of [Si], [P], and [S] on cell volume within diatom morphological types. Treatments: ambient nutrients (control), 2 nmol L⁻¹ Fe addition (+Fe), and 20 $\mu\text{mol L}^{-1}$ silicic acid addition (+Si).

acid concentrations were less silicified than SOAZ diatoms, whose uptake of silicic acid was saturated under ambient conditions. In two of three microcosm experiments, additions of silicic acid resulted in up to 50% increases in cellular Si content of the dominant diatom species [Baines *et al.*, 2010]. However, changes to cellular silicification actually declined on average across the experiments, largely because cell vol-

ume also increased after addition of silicic acid (Figure 4). At the whole community scale, silicification could not be related to surface silicic acid concentrations ($p = 0.44$). However, these concentrations varied only by a factor of three over the sampled portion of the EEP [Krause *et al.*, 2010a]. Additions of silicic acid had no effect on cellular S and P concentrations or content beyond that predicted by the change in cell volume.

Table 5. Regression Results for Predictions of Cellular Concentrations ($\text{mol } \mu\text{m}^{-3}$) of P ([P]_{cell}) and S ([S]_{cell}) in Diatoms Collected From the EEP^a

Response Variable	Equation	Parameter p Values	r^2
$\log[\text{Si}]_{\text{cell}}$	$+\mu_{\text{type}}; +\log(\text{volume}) \times -0.79 \pm 0.06; +\log([\text{Fe}]_{\text{aq}}) \times 0.01 \pm 0.05$	$<0.0001; <0.0001; <0.06$	0.87
$\log[\text{S}]_{\text{cell}}$	$+\mu_{\text{type}}; +\log(\text{volume}) \times -0.73 \pm 0.08; +\log([\text{Fe}]_{\text{aq}}) \times 0.39 \pm 0.07$	$<0.0001; <0.0001; <0.0001$	0.77
$\log[\text{P}]_{\text{cell}}$	$+\mu_{\text{type}}; +\log(\text{volume}) \times -0.7 \pm 0.12; +\log([\text{Fe}]_{\text{aq}}) \times 0.11 \pm 0.1$	$0.0006; <0.0001; 0.3$	0.58
$\log[\text{P}]_{\text{cell}}$	$+\mu_{\text{type}}; +\log([\text{S}]_{\text{cell}}) \times 0.84 \pm 0.08; +\log([\text{PO}_4]) \times 0.64 \pm 0.22$	$0.003; <0.0001; 0.006$	0.76

^aPredictors include morphological type (μ_{type}) and cell volume (μm^{-3}), as well as mixed layer average concentrations of dissolved Fe ($[\text{Fe}]_{\text{aq}}$, nmol L⁻¹) and phosphate ($[\text{PO}_4]$, $\mu\text{mol L}^{-1}$).

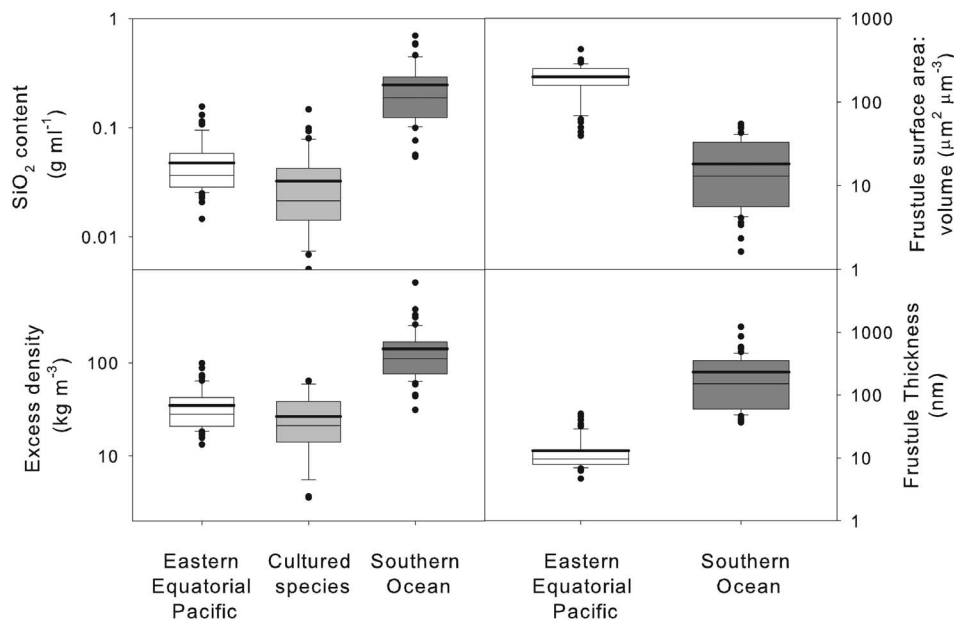


Figure 5. Differences between diatoms collected from the Southern Ocean and the eastern equatorial Pacific. The values for cultured cells are from (top left) *Conley et al.* [1989] and (bottom left) *Brzezinski* [1985]. Boxes enclose the 25th and 75th percentiles, the whiskers indicate the 10th and 90th percentiles, and closed circles are data lying outside the latter. The thin lines in the boxes are the median values and the thick lines are the mean values.

While ratios of Si:P and Si:S were consistently higher after silicic acid addition, the differences were not significant.

4. Discussion

[26] Silicification is a trait that is intrinsically linked to the unique role that diatoms play in the ocean due to its effects on density and composition of sinking particles. Our SXRF measurements show the diatom communities in two important Fe-limited regions of the ocean differ by a factor of six in their silicification. This difference is less indicative of poor silicification in the EEP diatoms than of high silicification in the SOAZ diatoms. The average Si content of diatom cells from the EEP was 50% higher than that predicted from biovolume using extant relationships [*Conley et al.*, 1989]. However, the average SOAZ diatom under Fe limitation was a factor of 11.3 ± 2.2 more silicified than cultured diatoms grown under nutrient replete conditions (Figure 5). In fact, the level of silicification observed for the SOAZ diatoms is more typical of cultured freshwater diatoms, which are on average an order of magnitude more silicified than cultured marine species [*Conley et al.*, 1989]. This finding underscores the importance of assessing field-collected phytoplankton contents rather than extrapolating from the mean composition of laboratory cultures.

[27] Ratios of Si to two proxies of organic matter (S and P) differed less between regions than did silicification. This pattern resulted from higher cellular concentrations of P and, to a lesser extent, S in the SOAZ than in the EEP. Differences in S and P content are not due to differences in cell size

between regions as regressions of C on biovolume predict that concentrations of cellular C should be 48% greater in the EEP than in the SOAZ (Table 2). The difference in P and S content could also not be attributed to higher Fe stress in the EEP, as proportional increases in cellular S and P concentrations after Fe addition were greater in the SOAZ than the EEP [*Baines et al.*, 2010; *Twining et al.*, 2004]. Higher cellular P concentrations in the SOAZ diatoms may have resulted in part from the fourfold higher phosphate concentrations there. Consistent with this hypothesis, cellular S:P ratios were lower in the SOAZ diatoms compared to those from the EEP (Table 4), and cellular P concentrations in the EEP were positively correlated with ambient phosphate concentrations (Table 5). However, the regional difference in cellular S content, the strong correlation of cellular P to cellular S, and response of cellular P to Fe addition suggest that much of the difference in cellular P was linked to a difference in organic matter content of the cells.

4.1. Comparisons to Other Data

[28] It is possible that we did not adequately characterize the communities we sampled due to inherent biases, or that the communities we sampled were not broadly representative of their respective regions. It is worth noting, therefore, that the cellular Si:P and Si:S ratios that we measure using SXRF are consistent with observed regional variations in the composition of particulate matter and changes in nutrient concentrations over time and depth (Table 4). In the SOAZ, for example, ratios of cellular Si:P approached 30 as diatoms came to dominate the plankton during one mesoscale Fe

addition [Hoffmann *et al.*, 2007], this value is similar to the Si:P ratio measured here after Fe addition (Table 4). Si:N use ratios after the SOFEX mesoscale Fe addition averaged 2.1 [Coale *et al.*, 2004], similar to the average ratio of 2.4 estimated for diatoms after Fe addition based on our SXRF data and assuming Redfield N:P stoichiometry (Table 4). Si:N ratios in Southern Ocean particulate matter when diatoms were dominant [Copin-Montegut and Copin-Montegut, 1978] and seasonal Si:N drawdown ratios [Brzezinski *et al.*, 2003] both average 4:1, similar to our estimate of cellular Si:N under low Fe. Likewise, ratios of net nitrate and silicic acid uptake that were determined from depth profiles in the Southern Ocean at latitudes between 55°S–70°S generally average 4.5 and range from 3 to 5.6 over all sectors of the Southern Ocean [Dunne *et al.*, 2007]. These nutrient use ratios have been attributed to more efficient recycling of organic nitrogen relative to silica [Brzezinski *et al.*, 2003] and to the effects of Fe limitation on diatom silicification and Si:N ratios [Dunne *et al.*, 2007; Sarmiento *et al.*, 2004]. While these factors must contribute to some extent, our data suggest that the high Si:N of the SOAZ diatoms must also play a role, and perhaps a dominant one.

[29] Because diatoms are rarer in the EEP, it is more difficult to make sensible comparisons between the SXRF measurements and field data on particulate matter and nutrient concentrations in this region. However, nutrient profiles and depletion of silicic acid and nitrate during mesoscale Fe additions suggest a much lower Si:N uptake ratio than exists in the SOAZ, in accordance with our findings (Table 4). During periods of rapid upwelling and high nitrate concentrations, diatoms appear to dominate export flux and new production [Dunne *et al.*, 1999]. Under these conditions silicic acid and nitrate are depleted at a ratio of 0.75–1.0 from upwelled waters by new production [Dugdale and Wilkerson, 1998; Dunne *et al.*, 1999]. Simultaneously measured ratios of Si and N in trap material near the equator (2°S to 2°N) are generally near 1, getting as high as 1.3 [Dunne *et al.*, 1999]. Likewise, as pennate diatoms similar to those measured here grew in response to Fe fertilization during IronEx II [Landry *et al.*, 2000], silicic acid and nitrate were depleted at a 1:1 ratio [Coale *et al.*, 1996]. Our measurements of cellular Si:P and Si:S in diatoms growing under low-Fe conditions suggest a Si:N ratio of nearly 1:1, in agreement with these field estimates (Table 4). Community nutrient use ratios in deckboard experiments, in which diatoms were primarily responsible for the increase in biomass in both controls and treatments [Brzezinski *et al.*, 2010], suggest slightly lower S:P and Si:N ratios under low-Fe conditions than estimated with SXRF (Table 4). A contribution of nondiatoms to the increase in biomass within the controls would tend to skew the Si:P and Si:N use ratios toward values lower than predicted by the measured Si:P in diatoms, as happens under field conditions [Dunne *et al.*, 1999]. Indeed, there was sometimes a measurable increase in chlorophyll in microcosms to which only Ge was added to inhibit diatom growth [Brzezinski *et al.*, 2010], indicating that nondiatoms also contributed to nutrient use in the controls. Uptake ratios in +Fe treatments, where diatoms dominated the response, were more similar to SXRF estimates (Table 4). While dissolved ammonia did not change substantially over the course of the experiments [Brzezinski

et al., 2010], assimilated nitrate may have been excreted as dissolved organic nitrogen, which was not assessed in these experiments. Such excretion can cause depletion ratios to underestimate measured cellular elemental composition. This mechanism has been used to explain similar overestimation of cellular N content via nitrate depletion in culture studies [Marchetti and Harrison, 2007].

4.2. Biogeochemical Implications of Differences in Silicification

[30] Silicification affects cell density, which in turn influences the sinking rate of aggregates and fecal pellets containing diatom cells or their remains. The cell-specific measurements of elemental content present a unique opportunity to assess the degree to which variability in silicification of diatoms can influence sinking rates of particles. We used the SXRF results and data obtained through microscopy to estimate the mass of three cellular fractions with distinct densities—the frustule, the cytoplasm and the vacuole—the sum of which was then divided by cell volume to get cell density (see Text S1 for details).¹ Mass of the frustule was determined by multiplying the SXRF measurement of cellular Si (mole cell⁻¹) by the hydrated molecular weight of opaline silica, which is assumed to be constant at ~67 g mol⁻¹ [Mortlock and Froelich, 1989]. For the cytoplasm mass, cellular carbon was first estimated from cellular S and P by assuming molar C:S and C:P ratios of 99 and 106 [Twining *et al.*, 2004], respectively, and the two estimates were averaged. We then assumed that C was 45% of the cell's dry mass [Parsons *et al.*, 1961] and that the ratio of wet mass to dry mass of cytoplasm was 3:1 as inferred from equations of Menden-Deuer and Lessard [2000] (see Text S1). To determine mass of the vacuole, the vacuole volume was determined by first calculating the frustules and cytoplasm volumes from their mass assuming densities of 2.15 g mL⁻¹ [Cummins, 1960] and 1.05 g mL⁻¹ [Reynolds, 2006], respectively, and then subtracting these volumes from the total cell volume. The mass of the vacuole was calculated assuming that its density was equivalent to that of the surrounding seawater at ambient temperature and salinity. Sensitivity analyses indicate that regional differences in excess density are robust to a wide range in variation in the assumed parameters, but very sensitive to cellular Si content (see Text S1).

[31] Our calculations suggest that the regional differences in silicification are likely to have substantial implications for particle sinking rates. Silica constitutes 34% of cellular wet mass in Fe limited SOAZ diatoms compared to 5.4% of the cellular wet mass of EEP diatoms. This sixfold difference in silica content caused the excess density (i.e., the difference between the density of the cell and that of the ambient water) to be larger by a factor of ~5 for Fe-limited diatoms from the SOAZ than for Fe-limited EEP diatoms (Figure 5). The excess density of empty frustules that are devoid of cytoplasm is estimated to differ by more than a factor of 7 between regions. Excess density of individual diatoms is imparted to the larger, faster sinking aggregates and fecal pellets that are the main vectors for the downward transport

¹Auxiliary materials are available with the HTML. doi:10.1029/2010GB003856.

of silica and carbon export from surface waters [Nelson *et al.*, 1995]. Taking into account temperature related differences in the viscosity of surface waters, our measurements suggest that aggregates and fecal pellets comprised entirely of intact diatom cells should sink by a factor of 2–3 faster in surface waters of the SOAZ (temp = 0°C, viscosity = 1.74 mPa sec) when compared to similarly sized aggregates in surface waters of the EEP (temp = 25°C, viscosity = 0.94 mPa sec). Because deep waters in both regions are similar in temperature, particle sinking rates at depth should differ in proportion to the relative difference in excess density, i.e., by a factor of ~5–7.

[32] The difference between the excess densities of diatoms and nondiatoms is also much larger in the SOAZ than in the EEP. Assuming that the density of cytoplasm in diatoms is identical to the density of nondiatom cells as a whole (1,050 g L⁻¹), diatoms in the EEP are estimated to have an excess density (38 g L⁻¹) that is only 50% greater than that of unballasted phytoplankton (27 g L⁻¹). Because diatoms are able to reduce their specific gravity by accumulating lipids [Smayda, 1970] and by regulating the ionic composition in the fluids of their large vacuoles [Gross and Zeuthen, 1948] the real excess density of living EEP diatoms is almost certainly lower than estimated here, possibly approaching that assumed for nondiatoms. In contrast, Fe-limited SOAZ diatoms exhibit excess densities that are a factor of 8 more than assumed for nondiatoms. In fact, they are so dense (1220 ± 40 g L⁻¹) that the cells would exhibit negative buoyancy even if the nonfrustule cell volume were entirely filled with lipid of density = 900 g L⁻¹. The difference between the excess densities of diatoms and nondiatoms in the SOAZ (164 g L⁻¹) is more than a factor of 15 greater than the same difference in the EEP (11 g L⁻¹). Because frustules may be crushed during ingestion, it is uncertain whether fecal pellets containing EEP or SOAZ diatoms would exhibit similar differences in excess density. Different packaging of cells within other types of aggregates could also offset the effect of the regional difference in silicification on particle sinking rates. These caveats aside, our results suggest that the efficiency of diatom export should be greater in the SOAZ than in the EEP.

[33] Our measurements also imply that the thinner frustules of EEP diatoms are likely to be far more susceptible to dissolution than those of heavily silicified SOAZ diatoms. Specific silica dissolution rates are proportional to the specific surface area of the frustules, which is the frustule surface area (SA_f) divided by the frustule volume (V_f) [Van Cappellen *et al.*, 2002]. To calculate SA_f, we first assume that the frustule is of even thickness and equivalent to the total cell volume minus a smaller volume of similar shape, which we call the nonfrustule volume. We then numerically solve for the difference in the linear dimensions of the frustule and nonfrustule volumes that cause the difference between them to equal the frustule volume estimated from SXRF (see Text S1 for details). Since dissolution of the silica can occur across the inner and outer surface of the frustules, we calculated frustule surface area as the sum of the outer cell surface area and the surface area of the nonfrustule volume. The mean SA_f:V_f for Fe-limited diatoms in the EEP is a factor of 16 ± 4 greater than in the SOAZ while the frustules of

SOAZ diatoms collected from low-Fe conditions are a factor of 21 ± 5 thicker than those of EEP diatoms (Figure 5).

[34] Our approach underestimates SA_f by ignoring frustule architecture and surface microtopography. Effective specific surface area measurements based on N₂ gas adsorption (BET method) yield values from 10 to 260 m² g⁻¹, with most values falling between 20 and 100 m² g⁻¹ [Dixit *et al.*, 2001]. Our estimates for SOAZ and EEP diatoms effectively bracket this range, averaging 5.6 and 98 m² g⁻¹, respectively. The EEP estimate is only twofold lower than the maximum values determined using other methods and similar to values of 95–139 m² g⁻¹ determined for a diatom assemblage collected from Hawaiian waters [Lawson *et al.*, 1978]. BET measurements on diatoms collected using net tows during SOFEX (mostly *Chaetoceros*) averaged 13 m² g⁻¹, again about twofold greater than our estimates [Demarest *et al.*, 2009]. The above comparisons suggest a twofold underestimation of specific surface area by our methods. However, these biases are modest compared to the 15-fold difference in specific surface area that we estimate for SOAZ and EEP diatoms. Moreover, the biases are similar in magnitude between regions. Indeed, SEM images of type specimens suggest that the predominant genera in our samples, *Fragilariopsis* and *Pseudonitzschia*, are structurally similar with little surface ornamentation [Round *et al.*, 2007]. Thus, we believe the relative difference in specific surface area between regions is robust to uncertainties in our estimate of specific surface area.

[35] Differences in the efficiency of biogenic silica and organic carbon export from surface waters of the EEP and SOAZ, and in the contribution of diatoms to these fluxes, are consistent with our estimated impact of silicification on sinking and regeneration of silica in surface waters. Estimates of the fractions of fixed carbon that are exported to depth are 0.06–0.12 in the EEP [Bacon *et al.*, 1996; Murray *et al.*, 1996] and 0.4–0.6 in the SOAZ [Moriceau *et al.*, 2007; Ragueneau *et al.*, 2002] – a factor of 3–10 difference. The factor of 2–7 difference in particle sinking rate that should result from the observed differences in diatom silicification is consistent with a difference of this magnitude if diatoms dominate the downward flux of materials in the SOAZ. Several lines of evidence suggest that diatoms do dominate vertical flux of particles in the SOAZ and that silica in diatoms is exported with much greater efficiency in the SOAZ than in the EEP. First, the fraction of biogenic silica production exported below the mixed layer is a factor of 4–6 larger in the SOAZ than in the EEP [Ragueneau *et al.*, 2002]. Second, while radiolarians always constitute a smaller fraction of plankton biomass than diatoms, they dominate the siliceous fraction of EEP sediments, which indicates the relatively high susceptibility of EEP diatom frustules to dissolution in the water column [Broecker and Peng, 1982]. Indeed, modeling studies suggest that nondiatoms must contribute substantially to the flux of carbon from surface waters in the EEP [Richardson *et al.*, 2004; Salihoglu and Hofmann, 2007]. Recent estimates indicate that diatoms are responsible for only 20% of the new production in the EEP [Krause *et al.*, 2010a]. In contrast, sediments in the SOAZ are dominated by diatom remains [Pondaven *et al.*, 2000]. While temperature-related differences in silica dissolution rates [Bidle *et al.*, 2002] or factors

that affect aggregation probabilities [Moriceau *et al.*, 2007] may also help to explain these patterns, the difference in silicification between the diatom assemblages that inhabit the SOAZ and EEP likely plays an important role and should be considered in biogeochemical models.

5. Conclusions

[36] Regional variation in silicification has not been as apparent previously because standard chemical methods cannot partition the elemental signatures of siliceous and nonsiliceous components of the plankton. Thus, variations in ratios of Si to other elements in particulate matter are more likely to reflect the relative abundance of diatoms to other nonsiliceous plankton than silicification of diatoms themselves. Given these constraints, scientists have been largely forced to assume that diatoms in the field have fixed ratios of Si to other elements and, by extension, fixed silica content. Where variation is allowed, it reflects a physiological response by an “ideal” diatom to factors such as available Fe and silicic acid [Mongin *et al.*, 2006]. These notions carry with them the additional presumption that differences between diatoms and other groups are relatively fixed. Here we have shown that large biogeochemically relevant regional differences in cellular silicification exist that are not observable except using cell-specific techniques. The differences in silicification do not appear to reflect short-term physiological responses to ambient conditions, including Fe and silicic acid concentrations. Rather, they reflect characteristics of the resident diatom communities as they have been shaped over time in response to the prevailing ecological, chemical and physical settings. Future efforts to understand the how the vertical flux of carbon is likely to respond to climate change, variation in dust deposition or ocean fertilization should consider how such factors may cause shifts in the characteristics of the diatom community that in turn affect the biogeochemical cycling of carbon and silicon.

[37] **Acknowledgments.** This work was funded by NSF grants to S.B.B., B.S.T., D.M.N., and N.S.F. (OCE 0527059, OCE 0527062). Use of the Advanced Photon Source was supported by the U.S. Department of Energy, Office of Science, Office of Basic Energy Sciences, under contract DE-AC02-06CH11357. Adrian Marchetti aided with identification of diatom species.

References

- Armstrong, R. A., C. Lee, J. I. Hedges, S. Honjo, and S. G. Wakeham (2002), A new, mechanistic model for organic carbon fluxes in the ocean based on the quantitative association of POC with ballast minerals, *Deep Sea Res., Part II*, 49, 219–236, doi:10.1016/S0967-0645(01)00101-1.
- Bacon, M. P., J. K. Cochran, D. Hirschberg, T. R. Hammar, and A. P. Flier (1996), Export flux of carbon at the equator during the EqPac time-series cruises estimated from Th-234 measurements, *Deep Sea Res., Part II*, 43, 1133–1153, doi:10.1016/0967-0645(96)00016-1.
- Baines, S. B., B. S. Twining, S. Vogt, W. M. Balch, N. S. Fisher, and D. M. Nelson (2010), Silicification of eastern equatorial Pacific diatoms exposed to additions of silicic acid and iron, *Deep Sea Res.*, doi:10.1016/j.dsr2.2010.08.003, in press.
- Bidle, K. D., M. Manganelli, and F. Azam (2002), Regulation of oceanic silicon and carbon preservation by temperature control on bacteria, *Science*, 298, 1980–1984, doi:10.1126/science.1076076.
- Broecker, W. S., and T. H. Peng (1982), *Tracers in the Sea*, Eldigio Press, New York.
- Brzezinski, M. A. (1985), The Si-C-N ratio of marine diatoms: Interspecific variability and the effect of some environmental variables, *J. Phycol.*, 21, 347–357, doi:10.1111/j.0022-3646.1985.00347.x.
- Brzezinski, M. A., M. L. Dickson, D. M. Nelson, and R. Sambrotto (2003), Ratios of Si, C and N uptake by microplankton in the Southern Ocean, *Deep Sea Res., Part II*, 50, 619–633, doi:10.1016/S0967-0645(02)00587-8.
- Brzezinski, M. A., et al. (2010), Co-limitation of diatoms by iron and silicic acid in the equatorial Pacific, *Deep Sea Res.*, doi:10.1016/j.dsr2.2010.08.005, in press.
- Buesseler, K. O. (1998), The decoupling of production and particulate export in the surface ocean, *Global Biogeochem. Cycles*, 12, 297–310, doi:10.1029/97GB03366.
- Chai, F., R. C. Dugdale, T. H. Peng, F. P. Wilkerson, and R. T. Barber (2002), One-dimensional ecosystem model of the equatorial Pacific upwelling system. Part I: Model development and silicon and nitrogen cycle, *Deep Sea Res., Part II*, 49, 2713–2745, doi:10.1016/S0967-0645(02)00055-3.
- Coale, K. H., et al. (1996), A massive phytoplankton bloom induced by an ecosystem-scale iron fertilization experiment in the equatorial Pacific Ocean, *Nature*, 383, 495–501, doi:10.1038/383495a0.
- Coale, K. H., et al. (2004), Southern Ocean iron enrichment experiment: Carbon cycling in high- and low-Si waters, *Science*, 304, 408–414, doi:10.1126/science.1089778.
- Conley, D. J., S. S. Kilham, and E. Theriot (1989), Differences in silica content between marine and fresh-water diatoms, *Limnol. Oceanogr.*, 34, 205–213, doi:10.4319/lo.1989.34.1.0205.
- Copin-Montegut, C., and G. Copin-Montegut (1978), The chemistry of particulate matter from the south Indian and Antarctic oceans, *Deep Sea Res.*, 25, 911–931, doi:10.1016/0146-6291(78)90633-1.
- Cummins, A. B. (1960), Diatomite, in *Industrial Minerals and Rocks (Nonmetallics Other Than Fuels)*, edited by J. L. Gillson, pp. 303–319, Am. Inst. of Mining, Metall., and Pet. Eng., New York.
- Demarest, M. S., M. A. Brzezinski, and C. P. Beucher (2009), Fractionation of silicon isotopes during biogenic silica dissolution, *Geochim. Cosmochim. Acta*, 73, 5572–5583, doi:10.1016/j.gca.2009.06.019.
- Dixit, S., P. Van Cappellen, and A. J. van Bennekom (2001), Processes controlling solubility of biogenic silica and pore water build-up of silicic acid in marine sediments, *Mar. Chem.*, 73, 333–352, doi:10.1016/S0304-4203(00)00118-3.
- Dugdale, R. C., and F. P. Wilkerson (1998), Silicate regulation of new production in the equatorial Pacific upwelling, *Nature*, 391, 270–273, doi:10.1038/34630.
- Dunne, J. P., J. W. Murray, A. K. Aufdenkampe, S. Blain, and M. Rodier (1999), Silicon-nitrogen coupling in the equatorial Pacific upwelling zone, *Global Biogeochem. Cycles*, 13, 715–726, doi:10.1029/1999GB900031.
- Dunne, J. P., J. L. Sarmiento, and A. Gnanadesikan (2007), A synthesis of global particle export from the surface ocean and cycling through the ocean interior and on the seafloor, *Global Biogeochem. Cycles*, 21, GB4006, doi:10.1029/2006GB002907.
- Foley, D. G., T. D. Dickey, M. J. McPhaden, R. R. Bidigare, M. R. Lewis, R. T. Barber, S. T. Lindley, C. Garside, D. V. Manov, and J. D. McNeil (1997), Longwaves and primary productivity variations in the equatorial Pacific at 0 degrees, 140 degrees W, *Deep Sea Res., Part II*, 44, 1801–1826, doi:10.1016/S0967-0645(97)00080-5.
- Franck, V. M., M. A. Brzezinski, K. H. Coale, and D. M. Nelson (2000), Iron and silicic acid concentrations regulate Si uptake north and south of the Polar Frontal Zone in the Pacific Sector of the Southern Ocean, *Deep Sea Res., Part II*, 47, 3315–3338, doi:10.1016/S0967-0645(00)00070-9.
- Franck, V. M., D. A. Hutchins, K. W. Bruland, and M. A. Brzezinski (2003), Iron and zinc effects on silicic acid and nitrate uptake kinetics in three high-nutrient, low-chlorophyll (HNLC) regions, *Mar. Ecol. Prog. Ser.*, 252, 15–33, doi:10.3354/meps252015.
- Gross, F., and E. Zeuthen (1948), The buoyancy of plankton diatoms: A problem of cell physiology, *Proc. R. Soc. London, Ser. B*, 135, 382–389, doi:10.1098/rspb.1948.0017.
- Hillebrand, H., C.-D. Durselen, D. Kirschtel, U. Pollinger, and T. Zohary (1999), Biovolume calculation for pelagic and benthic microalgae, *J. Phycol.*, 35, 403–424, doi:10.1046/j.1529-8817.1999.3520403.x.
- Hoffmann, L. J., I. Peeken, K. Lochte, P. Assmy, and M. Veldhuis (2006), Different reactions of Southern Ocean phytoplankton size classes to iron fertilization, *Limnol. Oceanogr.*, 51, 1217–1229, doi:10.4319/lo.2006.51.3.1217.

- Hoffmann, L. J., I. Peeken, and K. Lochte (2007), Effects of iron on the elemental stoichiometry during EIFEX and in the diatoms *Fragilariopsis kerguelensis* and *Chaetoceros dictyota*, *Biogeosciences*, *4*, 569–579, doi:10.5194/bg-4-569-2007.
- Hutchins, D. A., and K. W. Bruland (1998), Iron-limited diatom growth and Si: N uptake ratios in a coastal upwelling regime, *Nature*, *393*, 561–564, doi:10.1038/31203.
- Jin, X., N. Gruber, J. P. Dunne, J. L. Sarmiento, and R. A. Armstrong (2006), Diagnosing the contribution of phytoplankton functional groups to the production and export of particulate organic carbon, CaCO₃, and opal from global nutrient and alkalinity distributions, *Global Biogeochem. Cycles*, *20*, GB2015, doi:10.1029/2005GB002532.
- Krause, J. W., D. M. Nelson, and M. A. Brzezinski (2010a), Biogenic silica production and diatoms' contribution to primary and new production in the eastern equatorial Pacific, *Deep Sea Res.*, doi:10.1016/j.dsr2.2010.08.010, in press.
- Krause, J. W., M. A. Brzezinski, M. R. Landry, S. B. Baines, D. M. Nelson, K. E. Selph, A. G. Taylor, and B. S. Twining (2010b), The effects of biogenic silica detritus, zooplankton grazing, and diatom-size structure on Si-cycling in the euphotic zone of the eastern equatorial Pacific, *Limnol. Oceanogr.*, *55*, 2608–2622, doi:10.4319/lo.2010.55.6.2608.
- Landry, M. R., M. E. Ondrusek, S. J. Tanner, S. L. Brown, J. Constantinou, R. R. Bidigare, K. H. Coale, and S. Fitzwater (2000), Biological response to iron fertilization in the eastern equatorial Pacific (IronEx II). I. Microplankton community abundances and biomass, *Mar. Ecol. Prog. Ser.*, *201*, 27–42, doi:10.3354/meps201027.
- Lawson, D. S., D. C. Hurd, and H. S. Pankratz (1978), Silica dissolution rates of decomposing phytoplankton assemblages at various temperatures, *Am. J. Sci.*, *278*, 1373–1393, doi:10.2475/ajs.278.10.1373.
- Marchetti, A., and N. Cassar (2009), Diatom elemental and morphological changes in response to iron limitation: A brief review with potential paleoceanographic applications, *Geobiology*, *7*, 419–431, doi:10.1111/j.1472-4669.2009.00207.x.
- Marchetti, A., and P. J. Harrison (2007), Coupled changes in the cell morphology and the elemental (C, N, and Si) composition of the pennate diatom *Pseudo-nitzschia* due to iron deficiency, *Limnol. Oceanogr.*, *52*, 2270–2284.
- Marchetti, A., D. E. Varela, V. P. Lance, Z. Johnson, M. Palmucci, M. Giordano, and E. V. Armbrusta (2010), Iron and silicic acid effects on phytoplankton productivity, diversity and chemical composition in the central equatorial Pacific Ocean, *Limnol. Oceanogr.*, *55*, 11–29.
- Marinov, I., A. Gnanadesikan, J. R. Toggweiler, and J. L. Sarmiento (2006), The Southern Ocean biogeochemical divide, *Nature*, *441*, 964–967, doi:10.1038/nature04883.
- Menden-Deuer, S., and E. J. Lessard (2000), Carbon to volume relationships for dinoflagellates, diatoms, and other protist plankton, *Limnol. Oceanogr.*, *45*, 569–579.
- Mongin, M., D. M. Nelson, P. Pondaven, and P. Treguer (2006), Simulation of upper-ocean biogeochemistry with a flexible-composition phytoplankton model: C, N and Si cycling and Fe limitation in the Southern Ocean, *Deep Sea Res., Part II*, *53*, 601–619, doi:10.1016/j.dsr2.2006.01.021.
- Moore, J. K., S. C. Doney, and K. Lindsay (2004), Upper ocean ecosystem dynamics and iron cycling in a global three-dimensional model, *Global Biogeochem. Cycles*, *18*, GB4028, doi:10.1029/2004GB002220.
- Moriceau, B., M. Gallinari, K. Soetaert, and O. Ragueneau (2007), Importance of particle formation to reconstructed water column biogenic silica fluxes, *Global Biogeochem. Cycles*, *21*, GB3012, doi:10.1029/2006GB002814.
- Mortlock, R. A., and P. N. Froelich (1989), A simple method for the rapid determination of biogenic opal in pelagic marine sediments, *Deep Sea Res., Part I*, *36*, 1415–1426, doi:10.1016/0198-0149(89)90092-7.
- Murray, J. W., J. Young, J. Newton, J. Dunne, T. Chapin, B. Paul, and J. J. McCarthy (1996), Export flux of particulate organic carbon from the central equatorial Pacific determined using a combined drifting trap Th-234 approach, *Deep Sea Res., Part II*, *43*, 1095–1132, doi:10.1016/0967-0645(96)00036-7.
- Nelson, D. M., and M. R. Landry (2010), Complex regulation of phytoplankton productivity and upper-ocean biogeochemistry in the eastern equatorial Pacific: Introduction to results of the equatorial biocomplexity project, *Deep Sea Res.*, doi:10.1016/j.dsr2.2010.08.001, in press.
- Nelson, D. M., P. Treguer, M. A. Brzezinski, A. Leynaert, and B. Queguiner (1995), Production and dissolution of biogenic silica in the ocean: Revised global estimates, comparison with regional data and relationship to biogenic sedimentation, *Global Biogeochem. Cycles*, *9*, 359–372, doi:10.1029/95GB01070.
- Núñez-Milland, D. R., S. B. Baines, S. Vogt, and B. S. Twining (2010), Quantification of phosphorus in single cells using synchrotron X-ray fluorescence, *J. Synchrotron Radiat.*, *17*, 560–566, doi:10.1107/S0909049510014020.
- Paasche, E. (1973), Silicon and the ecology of marine diatoms: II. Silicate-uptake kinetics of five diatom species, *Mar. Biol. Berlin*, *19*, 262–269, doi:10.1007/BF02097147.
- Parsons, T. R., K. Stephens, and J. D. H. Strickland (1961), On the chemical composition of 11 species of marine phytoplankters, *J. Fish. Res. Board Can.*, *18*, 1001–1016.
- Pondaven, P., O. Ragueneau, P. Treguer, A. Hauvespre, L. Dezileau, and J. L. Reyss (2000), Resolving the 'opal paradox' in the Southern Ocean, *Nature*, *405*, 168–172, doi:10.1016/j.prots.2006.09.002.
- Ragueneau, O., N. Dittert, P. Pondaven, P. Treguer, and L. Corrin (2002), Si/C decoupling in the world ocean: Is the Southern Ocean different?, *Deep Sea Res., Part II*, *49*, 3127–3154, doi:10.1016/S0967-0645(02)00075-9.
- Reynolds, C. S. (2006), *Ecology of the Phytoplankton*, Cambridge, New York.
- Richardson, T. L., G. A. Jackson, H. W. Ducklow, and M. R. Roman (2004), Carbon fluxes through food webs of the eastern equatorial Pacific: An inverse approach, *Deep Sea Res., Part I*, *51*, 1245–1274, doi:10.1016/j.dsr.2004.05.005.
- Round, F. E., R. M. Crawford, and D. G. Mann (2007), *Diatoms: Biology and Morphology of the Genera*, Cambridge Univ. Press, Cambridge, U. K.
- Salihoglu, B., and E. E. Hofmann (2007), Simulations of phytoplankton species and carbon production in the equatorial Pacific Ocean: 1. Model configuration and ecosystem dynamics, *J. Mar. Res.*, *65*, 219–273.
- Sarmiento, J. L., N. Gruber, M. A. Brzezinski, and J. P. Dunne (2004), High-latitude controls of thermocline nutrients and low latitude biological productivity, *Nature*, *427*, 56–60, doi:10.1038/nature02127.
- Sarthou, G., K. R. Timmermans, S. Blain, and P. Treguer (2005), Growth physiology and fate of diatoms in the ocean: A review, *J. Sea Res.*, *53*, 25–42, doi:10.1016/j.seares.2004.01.007.
- Smayda, T. J. (1970), The suspension and sinking of phytoplankton in the sea, *Oceanogr. Mar. Biol. Ann. Rev.*, *8*, 353–414.
- Strutton, P. G., J. P. Ryan, and F. P. Chavez (2001), Enhanced chlorophyll associated with tropical instability waves in the equatorial Pacific, *Geophys. Res. Lett.*, *28*, 2005–2008, doi:10.1029/2000GL012166.
- Strutton, P. G., A. Palacz, R. C. Dugdale, F. Chai, A. Marchi, A. E. Parker, V. Hogue, and F. P. Wilkerson (2010), The impact of equatorial Pacific tropical instability waves on hydrography and nutrients: 2004–2005, *Deep Sea Res.*, doi:10.1016/j.dsr2.2010.08.015, in press.
- Takahashi, T., R. A. Feely, R. F. Weiss, R. H. Wanninkhof, D. W. Chipman, S. C. Sutherland, and T. T. Takahashi (1997), Global air-sea flux of CO₂: An estimate based on measurements of sea-air pCO₂ difference, *Proc. Natl. Acad. Sci. U. S. A.*, *94*, 8292–8299, doi:10.1073/pnas.94.16.8292.
- Takeda, S. (1998), Influence of iron availability on nutrient consumption ratio of diatoms in oceanic waters, *Nature*, *393*, 774–777, doi:10.1038/31674.
- Taylor, A. G., M. R. Landry, K. E. Selph, and E. J. Yang (2010), Biomass, size structure and depth distributions of the microbial community in the eastern equatorial Pacific, *Deep Sea Res.*, doi:10.1016/j.dsr2.2010.08.017, in press.
- Timmermans, K. R., and B. van der Wagt (2010), Variability in cell size, nutrient depletion, and growth rates of the Southern Ocean diatom *Fragilariopsis kerguelensis* (bacillariophyceae) after prolonged iron limitation, *J. Phycol.*, *46*, 497–506, doi:10.1111/j.1529-8817.2010.00827.x.
- Timmermans, K. R., B. van der Wagt, and H. J. W. de Baar (2004), Growth rates, half-saturation constants, and silicate, nitrate, and phosphate depletion in relation to iron availability of four large, open-ocean diatoms from the Southern Ocean, *Limnol. Oceanogr.*, *49*, 2141–2151, doi:10.4319/lo.2004.49.6.2141.
- Twining, B. S., S. B. Baines, N. S. Fisher, J. Maser, S. Vogt, C. Jacobsen, A. Tovar-Sanchez, and S. A. Sanudo-Wilhelmy (2003), Quantifying trace elements in individual aquatic protist cells with a synchrotron X-ray fluorescence microprobe, *Anal. Chem.*, *75*, 3806–3816, doi:10.1021/ac034227z.
- Twining, B. S., S. B. Baines, and N. S. Fisher (2004), Element stoichiometries of individual plankton cells collected during the Southern Ocean

- Iron Experiment (SOFeX), *Limnol. Oceanogr.*, *49*, 2115–2128, doi:10.4319/lo.2004.49.6.2115.
- Van Cappellen, P., S. Dixit, and J. van Beusekom (2002), Biogenic silica dissolution in the oceans: Reconciling experimental and field-based dissolution rates, *Global Biogeochem. Cycles*, *16*(4), 1075, doi:10.1029/2001GB001431.
- Vogt, S. (2003), MAPS: A set of software tools for analysis and visualization of 3D X-ray fluorescence data sets, *J. Phys. IV*, *104*, 635–638, doi:10.1051/jp4:20030160.
-
- S. B. Baines, Department of Ecology and Evolution, Stony Brook University, Stony Brook, NY 11794-5245, USA. (sbaines@ms.cc.sunysb.edu)
- M. A. Brzezinski, Marine Science Institute and the Department of Ecology, Evolution and Marine Biology, University of California, Santa Barbara, CA 93106, USA. (brzezins@lifesci.ucsb.edu)
- N. S. Fisher, School of Marine and Atmospheric Sciences, Stony Brook University, Stony Brook, NY 11794-5000, USA. (nfisher@notes.cc.sunysb.edu)
- D. M. Nelson, Institut Universitaire Européen de la Mer, Technopôle Brest-Iroise, Place Nicolas Copernic, F-29280 Plouzané, France. (david.nelson@univ-brest.fr)
- B. S. Twining, Bigelow Laboratory for Ocean Sciences, West Boothbay Harbor, ME 04575-0475, USA. (btwining@bigelow.org)